

Supplementary materials

Electric field-tuneable crossing of hole Zeeman splitting and orbital gaps in compressively strained germanium semiconductor on silicon

Maksym Myronov^{1*}, Philip Waldron², Pedro Barrios², Alex Bogan², Sergei Studenikin^{2*}

¹Physics Department, The University of Warwick, Coventry CV4 7AL, UK

²National Research Council of Canada, Ottawa, Ontario, Canada

Supplementary Note 1. Additional experimental data

To test our observations, we performed additional transport measurements on another gated Hall bar device made from the same epi wafer. The second Hall bar (HB) has different dimensions: the HB width is 20 μm , and the distance between potential probes is 60 μm . The device micro-photograph is shown in Fig. 1S.

Magnetotransport measurements on the second device were performed in a dilution refrigerator, equipped with an 18T superconducting solenoid magnet, at a temperature $T=125$ mK.



Figure 1S. A microphotograph of the second gated Hall bar sample, width of the HB channel 20 μm , and the distance between potential contacts 60 μm .

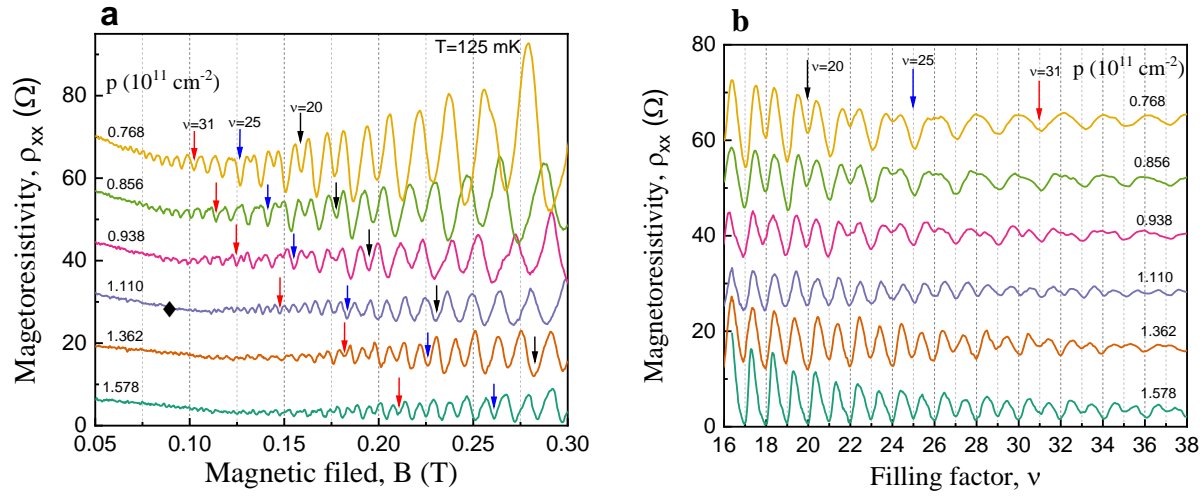


Figure 2S. **Magnetotransport characterisation of the second gated Hall bar device shown in Fig. 1S at $T=125$ mK.** The 2DHG areal densities are determined from the SdH oscillations period. The filling factor minima at $\nu = 20, 25,$ and 31 are indicated by the black, blue and red arrows, correspondingly. a) Magnetoconductivity traces as a function of the magnetic field, B. b) Magnetoconductivity traces as a function of filling factor, ν .

Figure 2S shows experimental traces of the magnetoconductivity as a function of the magnetic field (a) and the filling factor (b). The areal hole density was determined from the period of the SdH oscillations and controlled by the gate voltage. Carrier concentration is indicated by labels next to each trace. Several minima for different odd/even filling factors $\nu = 20, 25,$ and 31 are indicated by black, blue, and red arrows, correspondingly. Following the arrows from top (low density) to the bottom (large densities) the transition $E_{orb} \approx E_Z$ is evident around the middle curve marked in Fig. 2a by a black diamond. The results obtained on this narrow Hall bar are similar to those discussed in the main text, i.e. wider Hall bar. The critical transition $E_{orb} \approx E_Z$ governed by the g^* -factor tuneability occurs at a very similar carrier concentration $p \approx 10^{11} \text{ cm}^{-2}$ as for the wider Hall bar discussed in the main text.

Supplementary Note 2. An effect of possible effective mass dependence on the carrier concentration

It is known that the effective mass may depend on the carrier density due to Coulomb electron-electron or hole-hole, in our case, interactions^{1, 2} and/or due to variations of the valence band energy spectrum caused by the strong vertical electric field.³ However, the first mechanism results in a quite small variation of the effective mass of only a few per cents². The effective mass variation with the density $m^*(p)$ due to this mechanism is becoming more pronounced for very small carrier concentrations below $\sim 5 \times 10^{10} \text{ cm}^{-2}$, which is outside of the range of our study. In addition, the $m^*(p)$ dependence possesses a strongly non-linear character that would clearly be reflected in the results, that have not been detected in our experiments.

For the second mechanism³, the authors report on the hole effective mass variations measured at different hole densities. In fact, this change is due to strong electric field affecting the valence band energy spectrum, rather than a direct dependence of hole effective mass on the carrier density. The authors of this article, though, do not discuss the microscopic origin of the observed variation of m^* with the density. In the quoted paper by Lodari et al.³ the experiment was conducted in a very broad range of carrier density reaching $\sim 10^{12} \text{ cm}^{-2}$. Such large densities are produced by very large electric fields affecting the quantum well band bending and, correspondingly, the holes' band energy spectrum.^{4,5} Our experiments are performed in much smaller range carrier densities of $p \leq 1.5 \cdot 10^{11} \text{ cm}^{-2}$. This is an order of a magnitude smaller compared to Ref.³, therefore, we do not expect large change of the effective mass for different densities. A careful analysis of the $m^*(p)$ as a function of density in our experiments is masked by the large spin splitting effects, which becomes dominant for situations close to the critical transition $E_{orb} \approx E_Z$ for densities $p \approx 10^{11} \text{ cm}^{-2}$. To refute possible m^* variation with the density, that could effect the g^* -factor extraction procedure, it is important to note that in our experimental results we observe the critical transition from $E_{orb} > E_Z$, through the $E_{orb} = E_Z$, to $E_{orb} < E_Z$ that undoubtedly indicates that the g^* -factor variation occurs independently of the effective mass. If one assumes that g^* depends inversely on m^* , $\Delta g^* \propto 1/m^*$ (eq. (5) in Ref. ⁶, then in this situation such a crossover through the $E_{orb}=E_Z$ condition would be impossible to reach because m^* and g^* would change synchronously in the opposite directions keeping the ratio E_{orb}/E_Z approximately constant. This is because a larger effective mass would correspond to a smaller g^* -factor with $E_{orb} \propto \hbar\omega_c = \hbar eB/m^*$ and $E_{orb} \propto \hbar\omega_c = \hbar eB/m^*$, therefore, $\frac{\Delta E_{orb}}{\Delta E_Z} \sim \text{const}$ that would make it impossible to pass through the crossing.

Supplementary Note 3. Discussion of an effective g^* -factor anisotropy

It is known that effective g^* -factor in 2D hole systems is highly anisotropic with respect to the magnetic field direction^{7,8}. Such in-plane/out-of-plane anisotropy of hole g^* -factor was observed in various materials, e.g. in GaAs.^{9,10} In strained germanium the effective hole g^* -factor is also highly anisotropic as was reported in Ref.¹¹ The effective g^* -factor values below 1, for in-plane magnetic field, and exceeding 10, in the out of plane B -field direction, were observed. However, in the current manuscript we focus merely on the out of plane g^* -factor and its tuneability by a perpendicular electric field in a FET-like gated Hall bar device. In this configuration only out of the plane g^* -factor is tuneable and matters. In a contrary situation, discussed in large number of publications (e.g., see ^{10,12} and references therein) the effective g^* -factor tuneability in quantum dot (QD) devices is achieved by using local gates, when the 3D geometry of QD becomes important, in particular, for small nanostructures, e.g. fabricated from silicon or in germanium hut-wire nanostructures.^{13,14,15} Therefore, the 3D representation of g^* -factor is required by a 3x3 tensor.^{16,17}

There is a number of reports on the effective hole g^* -factor anisotropy in QD devices, in particular, in germanium hut-QDs¹⁸ and silicon MOS QDs¹⁹ which clearly manifest a 3D character of the g^* -factor, in which case a 3x3 tensor-presentation is required to describe experimental data in magnetic fields of different orientations.¹⁹ To summarise the above, different mechanisms of the effective g^* -factor tuneability in QDs by local gates were studied in the literature. In our article, let us emphasise, we research the material's g^* -factor in a large 2DHG planar device (not a QD device), which is fully determined by the material's structure stack and the vertical electric field produced by the planar gate. In this strongly pronounced 2D situation, the effective hole g^* -factor has a very strong anisotropy with

respect to the in-plane/out-of-plane magnetic field direction. A very small in-plane component of the 2DHG g^* -factor tensor (at least 10 times smaller compared to the out of plane component) is expected and measured for 2D hole structures^{7,9,11,20}. Therefore, in our work there is no need to introduce a tensor presentation of the g^* -factor. The anisotropic properties of the effective g^* -factor in our devices will be studied separately, which is outside of the scope of the current publication.

Supplementary Note 4. Previous methods to obtain effective g^* -factor

In Ref. by Lu et al.²¹ the authors estimate the effective g^* -factor using the standard temperature activation measurements of the SdH oscillations amplitude described by the Lifshitz-Kosevich formula^{1,22}. In Ref.⁶ by Drichko et al. the authors use the contactless acoustic method to measure the SdH oscillations in strongly quantising fields when R_{xx} can reach zero at the base temperature. They analyse the individual minima using the standard activation-energy approach $\sigma_1 \propto \exp\left(-\frac{\Delta}{2k_B T}\right)$.

Both approaches by Lu et al.²¹ and Drichko et al.⁶ suffer from possible systematic errors due to unknown Landau level (LL) width and its dependence on the magnetic field and the filling factor. It would be instructive to find another method that would eliminate this deficiency that is one of the main claims of our work.

In our article we present a new method to obtain the effective g^* -factor, which eliminates the magnetic field dependence of the LL width by using the ratio of the dingle plots for odd and even factor SdH waves in small magnetic fields, in the regime of large filling factors where semi-empirical approach using the Lifshitz-Kosevich equation is commonly used^{6,21,23,24}.

Supplementary References

- 1 Coleridge, P. T., Hayne, M., Zawadzki, P. & Sachrajda, A. S. Effective masses in high-mobility 2D electron gas structures. *Surface Science* **361–362**, 560-563 (1996). [https://doi.org/http://dx.doi.org/10.1016/0039-6028\(96\)00469-4](https://doi.org/http://dx.doi.org/10.1016/0039-6028(96)00469-4)
- 2 Tan, Y. W. *et al.* Measurements of the Density-Dependent Many-Body Electron Mass in Two Dimensional GaAs/AlGaAs Heterostructures. *Physical Review Letters* **94**, 016405 (2005).
- 3 Lodari, M. *et al.* Light effective hole mass in undoped Ge/SiGe quantum wells. *Physical Review B* **100**, 041304 (2019). <https://doi.org/10.1103/PhysRevB.100.041304>
- 4 Terrazos, L. A. *et al.* Theory of hole-spin qubits in strained germanium quantum dots. *Physical Review B* **103**, 125201 (2021). <https://doi.org/10.1103/PhysRevB.103.125201>
- 5 Wang, C.-A., Scappucci, G., Veldhorst, M. & Russ, M. in *arXiv:2208.04795 [cond-mat.mes-hall]* (2022).
- 6 Drichko, I. L. *et al.* Effective g factor of 2D holes in strained Ge quantum wells. *J. Appl. Phys.* **123** (2018). <https://doi.org/10.1063/1.5025413>
- 7 Dorozhkin, S. I. Shubnikov-de Haas oscillation beats and anisotropy of the g -factor in two-dimensional hole systems. *Solid State Communications* **72**, 211-214 (1989). [https://doi.org/http://dx.doi.org/10.1016/0038-1098\(89\)90525-5](https://doi.org/http://dx.doi.org/10.1016/0038-1098(89)90525-5)
- 8 Winkler, R. *Spin-Orbit Coupling Effects in Two-Dimensional Electron and Hole Systems*, Springer Tracts in Modern Physics. (Springer Berlin, 2003).
- 9 Bogan, A. *et al.* Consequences of Spin-Orbit Coupling at the Single Hole Level: Spin-Flip Tunneling and the Anisotropic g Factor. *Physical Review Letters* **118**, 167701-167705 (2017).

- 10 Studenikin, S. *et al.* Single-hole physics in GaAs/AlGaAs double quantum dot system with strong spin-orbit interaction. *Semiconductor Science and Technology* **36**, 053001 (2021).
- 11 Mizokuchi, R., Maurand, R., Vigneau, F., Myronov, M. & De Franceschi, S. Ballistic One-Dimensional Holes with Strong g-Factor Anisotropy in Germanium. *Nano Lett.* **18**, 4861-4865 (2018).
<https://doi.org/10.1021/acs.nanolett.8b01457>
- 12 Studenikin, S. *et al.* Electrically tunable effective g-factor of a single hole in a lateral GaAs/AlGaAs quantum dot. *Communications Physics* **2**, 159 (2019). <https://doi.org/10.1038/s42005-019-0262-1>
- 13 Burkard, G., Ladd, T. D., Pan, A., Nichol, J. M. & Petta, J. R. Semiconductor spin qubits. *Rev. Mod. Phys.* **95**, 025003 (2023). <https://doi.org/10.1103/RevModPhys.95.025003>
- 14 Maurand, R. *et al.* A CMOS silicon spin qubit. *Nature Communications* **7**, 13575 (2016).
<https://doi.org/10.1038/ncomms13575>
<http://www.nature.com/articles/ncomms13575#supplementary-information>
- 15 Vukušić, L., Kukučka, J., Watzinger, H. & Katsaros, G. Fast Hole Tunneling Times in Germanium Hut Wires Probed by Single-Shot Reflectometry. *Nano Letters* **17**, 5706-5710 (2017).
<https://doi.org/10.1021/acs.nanolett.7b02627>
- 16 Crippa, A. *et al.* Electrical Spin Driving by g -Matrix Modulation in Spin-Orbit Qubits. *Physical Review Letters* **120**, 137702 (2018). <https://doi.org/10.1103/PhysRevLett.120.137702>
- 17 Maurand, R. *et al.* A CMOS silicon spin qubit. *Nature Communications* **7**, 6 (2016).
<https://doi.org/10.1038/ncomms13575>
- 18 Giorgioni, A. *et al.* Strong confinement-induced engineering of the g factor and lifetime of conduction electron spins in Ge quantum wells. *Nature Communications* **7**, 13886 (2016).
<https://doi.org/10.1038/ncomms13886>
- 19 Liles, S. D. *et al.* Electrical control of the g tensor of the first hole in a silicon MOS quantum dot. *Physical Review B* **104**, 235303 (2021). <https://doi.org/10.1103/PhysRevB.104.235303>
- 20 Srinivasan, A. *et al.* Using a Tunable Quantum Wire To Measure the Large out-of-Plane Spin Splitting of Quasi Two-Dimensional Holes in a GaAs Nanostructure. *Nano Letters* **13**, 148-152 (2013).
<https://doi.org/10.1021/nl303596s>
- 21 Lu, T. M. *et al.* Effective g factor of low-density two-dimensional holes in a Ge quantum well. *Appl. Phys. Lett.* **111**, 102108 (2017). <https://doi.org/10.1063/1.4990569>
- 22 Isihara, A. & Smrcka, L. Density and magnetic field dependences of the conductivity of two-dimensional electron systems. *Journal of Physics C: Solid State Physics* **19**, 6777 (1986).
<https://doi.org/10.1088/0022-3719/19/34/015>
- 23 Coleridge, P. T., Stoner, R. & Fletcher, R. Low-field transport coefficients in GaAs/Ga_{1-x}Al_xAs heterostructures. *Phys. Rev. B* **39**, 1120-1124 (1989).
- 24 Sammak, A. *et al.* Shallow and Undoped Germanium Quantum Wells: A Playground for Spin and Hybrid Quantum Technology. *Advanced Functional Materials* **29**, 1807613 (2019).
<https://doi.org/https://doi.org/10.1002/adfm.201807613>